Eur. Phys. J. C 33, 523–536 (2004)
Digital Object Identifier (DOI) 10.1140/epjc/s2004-01603-2

THE EUROPEAN PHYSICAL JOURNAL C

Searching for dominant rescattering sources in decays of B to two pseudoscalars

C. Smith[a]

Institut de Physique Théorique, Université catholique de Louvain, Chemin du Cyclotron, 2, 1348, Louvain-la-Neuve, Belgium

Received: 15 September 2003 /
Published online: 3 March 2004 –

Abstract. Various rescattering sources are analyzed in the context of the $SU(3)$ flavor symmetry. In particular, the possibility to account for intermediate charm at the hadronic level in B to PP is thoroughly investigated. Then, the rescattering sources are compared in light of recent decay measurements of B to two charmless pseudoscalars, with emphasis on the size of strong phases and on patterns of direct CP-asymmetries.

1 Introduction

Studies of CP violation in the B system offer a unique window into the intimate structure of the standard model, and possibly give hints about new physics. The dedicated experiments at Cornell, KEK and SLAC have begun to feed theorists with precise data to test the current understanding of CP violation as well as alternate theories.

Recently, a number of rare hadronic decays B to two charmless pseudoscalars have been measured [1–6]. These modes are interesting for attempts to constrain the weak angle γ of the unitary triangle. However, for this program to be achieved, theoretical control is needed over the strong final state interactions (FSI). In the present work, this problem is addressed phenomenologically, at the hadronic level (for other approaches, see for example [7]). The basic tools are flavor symmetries like isospin or $SU(3)$ (see for example [8–10]) and Watson's theorem, or elasticity, for strong FSI [10–12].

Up to now, a serious shortcoming of elasticity-based approaches was their inability to account for intermediate charm. In short-distance analyses, quark diagrams involving charm quarks do have non-negligible imaginary parts [13]. This led to the common belief that rescattering cannot be elastic. One purpose of the present paper is to show that it is possible within the hadronic framework of Watson's theorem for elasticity to account for intermediate charm. Some results in that direction were already presented earlier [12]. Here, we will revert to the language of the usual quark diagram topologies. The theoretical foundations of our parameterization, which are articulated around a factorization property for FSI, are reviewed in the first part of the paper.

Another problem of elasticity-based approaches is that large strong phases are apparently required by current experimental data for decays of B to two charmless pseudoscalars (see for example [14]). This is in disagreement with Regge computations [15], with the expectation for two particles flying apart with high momentum [16] and with QCD-factorization predictions [17]. In the second part of this paper, we will show that, when intermediate charm is accounted for, the strong phases tend to be much smaller.

Finally, the last goal of this paper is to parameterize and quantify the corrections to the patterns for $B \to \pi K$ direct CP-asymmetries presented in [12]. These patterns were designed to discriminate among dominant rescattering sources, and we will here show that this capability is not altered.

2 Theoretical framework

The starting point of our analysis is the "generalized Watson theorem" (for details, see [10–12]), which permits the factorization of weak decay amplitudes into a factor invariant under CP and a factor that gets complex conjugated under CP:

$$W = \sqrt{S} W_{\rm b}, \tag{1a}$$

$$CP\,(W) = \sqrt{S} W_{\rm b}^{*}, \tag{1b}$$

where W is a vector containing the full decay amplitudes. Consequently, the real (up to CKM factors) $W_{\rm b}$ is identified as the *bare decay amplitude* (i.e. before FSI) denoted

$$W = \begin{pmatrix} B \to X_1 \\ \vdots \end{pmatrix}, \quad W_b = \begin{pmatrix} B \to \{X_1\} \\ \vdots \end{pmatrix}. \tag{2}$$

The unitary *rescattering matrix* $\sqrt{S}$ contains all the CP-conserving strong phases and describes final state interac-

[a] e-mail: smith@fyma.ucl.ac.be

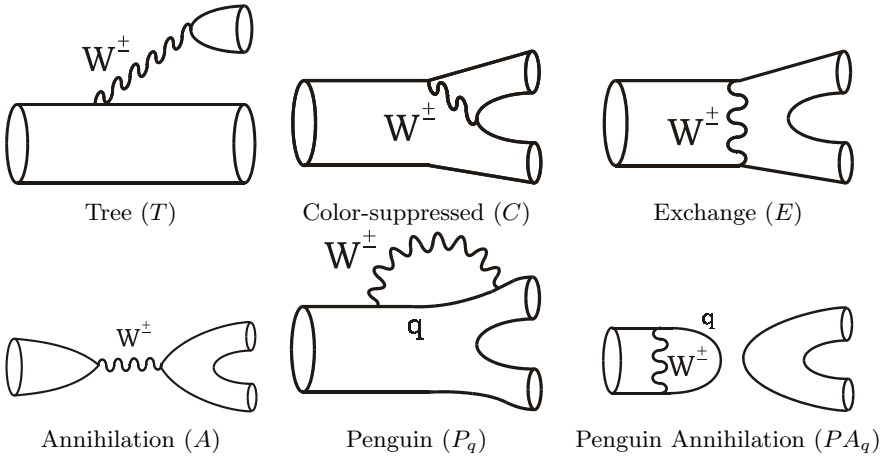

Fig. 1. Quark diagrams for non-singlet final states, $q = u, c, t$

tions (FSI). In general, one defines the rescattering *eigenchannels* C_i,

$$\begin{pmatrix} C_1 \\ \vdots \end{pmatrix} = O_C \begin{pmatrix} \{X_1\} \\ \vdots \end{pmatrix}, \tag{3}$$

as the basis in which $\sqrt{S}$ is diagonal:

$$S_{\text{diag}} = O_C.S.O_C^{\text{t}} = \begin{pmatrix} \mathrm{e}^{2\mathrm{i}\delta_{C_1}} & 0 & \cdots \\ 0 & \mathrm{e}^{2\mathrm{i}\delta_{C_2}} & \cdots \\ \vdots & \vdots & \ddots \end{pmatrix}, \tag{4}$$

with strong phases (or rescattering *eigenphases*) δ_{C_i} as diagonal elements. *Elasticity* (sometimes referred to as "quasi-elasticity") is defined as the conservation of the total decay probability, which follows from the unitarity of $\sqrt{S}$:

$$\|W\|^2 = \left\|\sqrt{S}W_b\right\|^2 = \|W_b\|^2 . \tag{5}$$

Assuming that CP and CPT hold for the strong interactions generating $\sqrt{S}$ implies that O_C is orthogonal (up to some phase conventions) since then $\sqrt{S}$ is unitary and symmetric. The angles parameterizing O_C are then called *mixing angles* since they govern the FSI mixings among decay channels.

In principle, $\sqrt{S}$ should be a $n \times n$ matrix with n the number of B-meson decay channels which can be connected by strong interactions. In practice, however, we expect that to a good approximation this matrix is block-diagonal. Unfortunately, it is not known at present how large the extent of each block should be to capture the essential rescattering physics. In the present work, we assume that two-body $\rightleftharpoons$ n-body rescatterings are negligible (as could be justified from $1/N$ arguments [18]), or at least suppressed by large cancellations.

The most restrictive (though non-trivial) approximation is that of $SU(2)$-elasticity: each block of $\sqrt{S}$ corresponds to an isospin multiplet, which means that only rescatterings like $\pi\pi \rightleftharpoons \pi\pi$ or $K\bar{K} \rightleftharpoons K\bar{K}$ [12] are allowed. A more flexible approach is to consider $SU(3)$-elasticity, to open rescatterings between different isomultiplets like $\pi\pi \rightleftharpoons K\bar{K}$ or $\pi K \rightleftharpoons \eta_8 K$. In an attempt to capture all the relevant physics, rescattering channels like $D\bar{D} \rightleftharpoons \pi\pi$ or $D_s\bar{D} \rightleftharpoons \pi K$ should also be opened to account for intermediate charm. However, sizable $D\bar{D} \rightleftharpoons PP$ rescatterings like those implied by $SU(4)$-elasticity would average decay amplitudes and produce $\mathrm{Br}\left(B \to D\bar{D}\right) \sim \mathrm{Br}\left(B \to PP\right)$, in clear disagreement with experiment

$$\mathrm{Br}^{\text{exp}}\left(B \to D_s\bar{D}\right) \sim 10^{-2} \gg \mathrm{Br}^{\text{exp}}\left(B \to K\pi\right) \sim 10^{-5}. \tag{6}$$

Intermediate charm rescattering effects are thus quite small, and can be accounted for as distortions of $SU(3)$-elasticity. We call *enlarged* $SU(3)$-elasticity this parameterization of FSI, since the $SU(3)$ flavor symmetry remains exact. Conversely, even if all the rescatterings (both two-body and multi-body) are small, the $D\bar{D} \rightleftharpoons PP$ ones may still lead to sizable effects because of (6), so it is desirable to have an adequate formalism at hand.

By definition, bare amplitudes W_{b} are real (except for CKM matrix elements) since they do not contain any FSI effects (see (1)). To parameterize them, and to make contact with the short-distance weak decay of the b quark, it is convenient to introduce quark diagrams which account for the possible flavor flows (see, for example, [8–10]). To first order in the weak interactions, and to all orders in the strong interactions (except FSI), the six topologies needed for $B \to \{PP\}$, $P = \pi, K, \eta_8$ and $B \to \left\{D\bar{D}\right\}$, $D = D, D_s$ are shown in Fig. 1.

In principle, second-order weak interaction topologies are very small, except for those depicted in Fig. 2 involving an enhancement factor m_{top}^2/M_Z^2.

The $SU(3)$ symmetry is implemented at the level of bare decay amplitudes by identifying quark diagrams that differ only by the interchange $u \leftrightarrow d \leftrightarrow s$. The badly broken $SU(4)$ symmetry is not invoked and, consequently, quark diagrams for $B \to \left\{D\bar{D}\right\}$ will be distinguished from $B \to \{PP\}$ ones by a subscript D.

Rescattering matrices have an interesting property of factorization. If each of the strong phases is expressed as

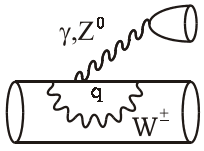

Electroweak Penguin (P_q^{EW})

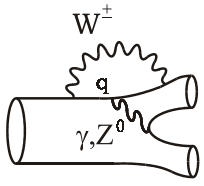

Color-suppressed Electroweak Penguin ($P_{C,q}^{EW}$)

Fig. 2. Second-order weak interaction quark diagrams

the sum of two parts,

$$\delta_{C_i} = \delta^a_{C_i} + \delta^b_{C_i} \ , \tag{7}$$

then, from the unitarity of $\sqrt{S}$ (see (4))

$$\sqrt{S}\,(\delta_{C_1}, ...) = \sqrt{S}(\delta^a_{C_1}, ...)\,.\,\sqrt{S}(\delta^b_{C_1}, ...). \tag{8}$$

Now, we can define *effective* "bare" amplitudes containing the $\delta^b_{C_i}$ part of the CP-conserving strong phases:

$$W = \sqrt{S}\,(\delta_{C_1}, ...)\ .W_{\rm b} \equiv \sqrt{S}(\delta^a_{C_1}, ...)\,.W^{\rm eff}_{\rm b}. \tag{9}$$

In just the same way $W_{\rm b}$ is parameterized in terms of real bare quark diagrams T, C,..., the effective bare amplitudes $W^{\rm eff}_{\rm b}$ are decomposed into complex effective quark diagram amplitudes $T^{\rm eff}, C^{\rm eff}, ...$ (i.e. $W^{\rm eff}_{\rm b} = W_{\rm b}\left(T \to T^{\rm eff}, C \to C^{\rm eff}, ...\right)$). It is important to realize that, in the literature, quark diagrams are often introduced at the level of $W^{\rm eff}_{\rm b}$. One should then be very careful in understanding which part of the FSI they contain, so that different approaches can be related. Finally, note that $CP(W^{\rm eff}_{\rm b}) \neq (W^{\rm eff}_{\rm b})^*$ since some CP-invariant strong phases are now included into them (compare with (1)).

2.1 $SU(3)$-elastic rescattering

$SU(3)$-elasticity is enforced by taking definite $SU(3)$ states as rescattering eigenchannels. Taking as an example the set of decay amplitudes

$$W = \begin{pmatrix} B^+ \to K^+\eta_8 \\ B^+ \to K^+\pi^0 \\ B^+ \to K^0\pi^+ \\ B^+ \to D_s^+\bar{D}^0 \end{pmatrix}, \tag{10}$$

the rescattering matrix S is diagonal:

$$S_{\rm diag} = {\rm diag}\left({\rm e}^{2{\rm i}\delta_{27}}, {\rm e}^{2{\rm i}\delta_{27}}, {\rm e}^{2{\rm i}\delta_8}, {\rm e}^{2{\rm i}\delta_8^D}\right), \tag{11}$$

in the basis defined by

$$\begin{pmatrix} |27,3/2,1/2,1\rangle \\ |27,1/2,1/2,1\rangle \\ |8,1/2,1/2,1\rangle \\ |8_D,1/2,1/2,1\rangle \end{pmatrix} = \begin{pmatrix} 0 & -\sqrt{\frac{2}{3}} & \frac{1}{\sqrt{3}} & 0 \\ -\frac{3}{\sqrt{10}} & -\frac{1}{\sqrt{30}} & -\frac{1}{\sqrt{15}} & 0 \\ \frac{1}{\sqrt{10}} & -\sqrt{\frac{3}{10}} & -\sqrt{\frac{3}{5}} & 0 \\ 0 & 0 & 0 & 1 \end{pmatrix} \begin{pmatrix} \{K^+\eta_8\} \\ \{K^+\pi^0\} \\ \{K^0\pi^+\} \\ \{D_s^+\bar{D}^0\} \end{pmatrix}. \tag{12}$$

Therefore, the $SU(3)$-elastic rescattering matrix is

$$\sqrt{S_{SU(3)}} = \begin{pmatrix} \frac{9{\rm e}^{2{\rm i}\delta_{27}}+{\rm e}^{2{\rm i}\delta_8}}{10} & \frac{\sqrt{3}\left({\rm e}^{2{\rm i}\delta_{27}}-{\rm e}^{2{\rm i}\delta_8}\right)}{10} & \frac{\sqrt{3}\left({\rm e}^{2{\rm i}\delta_{27}}-{\rm e}^{2{\rm i}\delta_8}\right)}{\sqrt{50}} & 0 \\ \frac{\sqrt{3}\left({\rm e}^{2{\rm i}\delta_{27}}-{\rm e}^{2{\rm i}\delta_8}\right)}{10} & \frac{7{\rm e}^{2{\rm i}\delta_{27}}+3{\rm e}^{2{\rm i}\delta_8}}{10} & \frac{3\left({\rm e}^{2{\rm i}\delta_8}-{\rm e}^{2{\rm i}\delta_{27}}\right)}{\sqrt{50}} & 0 \\ \frac{\sqrt{3}\left({\rm e}^{2{\rm i}\delta_{27}}-{\rm e}^{2{\rm i}\delta_8}\right)}{\sqrt{50}} & \frac{3\left({\rm e}^{2{\rm i}\delta_8}-{\rm e}^{2{\rm i}\delta_{27}}\right)}{\sqrt{50}} & \frac{2{\rm e}^{2{\rm i}\delta_{27}}+3{\rm e}^{2{\rm i}\delta_8}}{5} & 0 \\ 0 & 0 & 0 & {\rm e}^{2{\rm i}\delta_8^D} \end{pmatrix}. \tag{13}$$

See how $SU(3)$-elasticity fixes both the eigenphases (11) *and* the eigenchannels (12): the $\left\{D_s^+\bar{D}^0\right\}$ and $\{PP\}$ channels are not coupled and $\sqrt{S_{SU(3)}}$ has a characteristic block-diagonal form. Other sets of states are treated similarly [10].

Let us now concentrate on the $PP \rightleftharpoons PP$ part of $\sqrt{S_{SU(3)}}$. If each strong phase is expressed as $\delta_i = \delta_i^l + \delta_i^s$ with $i = 1, 8, 27$ (one could think of the FSI short and long-distance parts), we can define effective, complex quark diagrams by absorbing the δ_i^s part of the rescattering

$$W^{\rm eff}_{\rm b} = \sqrt{S_{SU(3)}}\,(\delta^s_{27}, \delta^s_8, \delta^s_1)\,W_{\rm b}. \tag{14}$$

Explicitly, effective quark diagrams can be expressed in terms of bare (real) ones as (omitting electroweak penguins for now)

$SU(3)$-elasticity:

$$\begin{cases} X^{\rm eff} = X{\rm e}^{{\rm i}\delta^s_8} + \frac{{\rm e}^{{\rm i}\delta^s_{27}}-{\rm e}^{{\rm i}\delta^s_8}}{2}\,(T+C) & X = T, C, \\ Y^{\rm eff} = Y{\rm e}^{{\rm i}\delta^s_8} - \frac{{\rm e}^{{\rm i}\delta^s_{27}}-{\rm e}^{{\rm i}\delta^s_8}}{10}\,(T+C) & Y = E, A, P_u, \\ P^{\rm eff}_{c,t} = P_{c,t}{\rm e}^{{\rm i}\delta^s_8}, & \\ PA^{\rm eff}_u = PA_u{\rm e}^{{\rm i}\delta^s_1} - \frac{{\rm e}^{{\rm i}\delta^s_{27}}-{\rm e}^{{\rm i}\delta^s_8}}{20}\,(T+C) & \\ \quad + \frac{{\rm e}^{{\rm i}\delta^s_1}-{\rm e}^{{\rm i}\delta^s_8}}{12}\,(3T - C + 8E + 8P_u)\,, & \\ PA^{\rm eff}_{c,t} = PA_{c,t}{\rm e}^{{\rm i}\delta^s_1} + \frac{2({\rm e}^{{\rm i}\delta^s_1}-{\rm e}^{{\rm i}\delta^s_8})}{3}P_{c,t}. & \end{cases} \tag{15}$$

The remaining δ_i^l part of the rescattering is accounted for by acting with $\sqrt{S_{SU(3)}}\left(\delta^l_{27}, \delta^l_8, \delta^l_1\right)$ on $W^{\rm eff}_{\rm b}$.

In the following, we shall not use (15). What we want to point out by writing them is that one should be careful when dealing with effective quark diagrams since, obviously, the rough scalings (penguins are discussed in the next section)

$$1\ : T,$$

$$\begin{aligned}\mathcal{O}(\lambda) &: C,\\ \mathcal{O}(\lambda^2) &: E, A,\end{aligned} \tag{16}$$

with $\lambda \approx 1/5$ [9], may no longer be valid. For example, for the $B^+ \to K^0\pi^+$ mode, while A is helicity-suppressed and can be safely ignored, $A^{\rm eff}$ receives unsuppressed contributions from T (provided $\delta_{27}^s - \delta_8^s$ is non-negligible), as already emphasized in [19]. Similarly, for $B^0 \to \pi^+\pi^-$, E and PA can be neglected, but $E^{\rm eff}$ and $PA^{\rm eff}$ may not. Equations (15) illustrate in the specific $SU(3)$-elastic case a more general fact: if one starts with a parameterization in terms of effective quark diagrams without specifying anything about FSI, all the effective quark diagrams are then arbitrary complex numbers and this costs much in terms of free parameters (except, of course, if one has a definite computation scheme for effective quark diagrams).

2.2 Intermediate charm rescattering

We now open the rescattering channel $D\bar{D} \rightleftharpoons PP$[1]. For the set of states (10), general rescattering eigenchannels are defined by mixing 8 with 8_D (for a discussion of the formalism used here, see [10,12]):

$$\begin{pmatrix} C_1\,(27,3/2)\\ C_2\,(27,1/2)\\ C_3\,(8,1/2)\\ C_4\,(8,1/2)\end{pmatrix} = \begin{pmatrix} 1 & 0 & 0 & 0\\ 0 & 1 & 0 & 0\\ 0 & 0 & \cos\chi_8 & \sin\chi_8\\ 0 & 0 & -\sin\chi_8 & \cos\chi_8\end{pmatrix} \begin{pmatrix} |27,3/2,1/2,1\rangle\\ |27,1/2,1/2,1\rangle\\ |8,1/2,1/2,1\rangle\\ |8_D,1/2,1/2,1\rangle\end{pmatrix}. \tag{17}$$

The rescattering matrix in the C_i basis is

$$\begin{aligned} S_{\rm diag} &= {\rm diag}\left(\mathrm{e}^{2\mathrm{i}\delta_{C_1}}, \mathrm{e}^{2\mathrm{i}\delta_{C_2}}, \mathrm{e}^{2\mathrm{i}\delta_{C_3}}, \mathrm{e}^{2\mathrm{i}\delta_{C_4}}\right)\\ &\approx {\rm diag}\left(\mathrm{e}^{2\mathrm{i}\delta_{27}}, \mathrm{e}^{2\mathrm{i}\delta_{27}}, \mathrm{e}^{2\mathrm{i}\delta_8}, \mathrm{e}^{2\mathrm{i}\delta_8^D}\right), \end{aligned} \tag{18}$$

since the mixing angle χ_8 should be small (see (6)). In the physical state basis, we then find

$$\begin{aligned}\sqrt{S_{\chi_8}} &= \sqrt{S_{SU(3)}}\\ &+ \sin(2\chi_8)\,\frac{\mathrm{e}^{\mathrm{i}\delta_8} - \mathrm{e}^{\mathrm{i}\delta_8^D}}{2\sqrt{10}} \begin{pmatrix} 0 & 0 & 0 & 1\\ 0 & 0 & 0 & -\sqrt{3}\\ 0 & 0 & 0 & -\sqrt{6}\\ 1 & -\sqrt{3} & -\sqrt{6} & 0\end{pmatrix}\\ &+ \sin^2(\chi_8)\,\frac{\mathrm{e}^{\mathrm{i}\delta_8} - \mathrm{e}^{\mathrm{i}\delta_8^D}}{10} \begin{pmatrix} -1 & \sqrt{3} & \sqrt{6} & 0\\ \sqrt{3} & -3 & -3\sqrt{2} & 0\\ \sqrt{6} & -3\sqrt{2} & -6 & 0\\ 0 & 0 & 0 & 10\end{pmatrix}, \end{aligned} \tag{19}$$

with $\sqrt{S_{SU(3)}}$ given in (13). In physical terms, one can understand χ_8 as a $D\bar{D}$–PP "coupling constant": the $\sin(2\chi_8)$ term describes the $D\bar{D}$ pollution of PP states (which proceeds through $D\bar{D} \overset{\chi_8}{\to} PP, D\bar{D} \overset{\chi_8}{\to} PP \overset{\chi_8}{\to} D\bar{D} \overset{\chi_8}{\to} PP$, etc.) while the $\sin^2(\chi_8)$ terms account for "inelastic" distortion of the rescattering among $\{PP\}$ states due to the exchange of probability with the $D\bar{D}$ channel ($PP \overset{\chi_8}{\to} D\bar{D} \overset{\chi_8}{\to} PP$, etc). The common factor $\mathrm{e}^{\mathrm{i}\delta_8} - \mathrm{e}^{\mathrm{i}\delta_8^D}$ acts as a kinematical suppression since it decreases as the relative momentum between decay products increases ($\delta_8 = \delta_8^D = 0$ in the limit $M_B \to \infty$ [16]). Finally, note well that $SU(3)$ remains exact, and that the rescattering is elastic (conserved total probability) for the full set of states $\{PP, D\bar{D}\}$ since $\sqrt{S_{\chi_8}}$ is unitary for all χ_8.

Other sets of states are treated similarly (the mixings among $Y = 0, T_3 = 0$ states is described in Appendix A). All in all, six parameters are needed to describe all the rescattering mixings (one of the strong phase can be eliminated)

$$\begin{aligned} PP: (8\otimes 8)_S = &\\ 27 \quad &\oplus \quad 8 \quad \oplus \quad 1 \quad \to \delta_{27}, \delta_8, \delta_1,\\ &\quad \updownarrow \chi_8 \quad \updownarrow \chi_1\\ D\bar{D}: \ 3\otimes\bar{3} \ = &\\ &\quad 8_D \quad \oplus \quad 1_D \quad \to \delta_8^D, \delta_1^D. \end{aligned} \tag{20}$$

We expect that $\chi_8, \chi_1 \ll 1$ since $D\bar{D} \to PP$ proceeds through the annihilation of the $c\bar{c}$ pair into light quarks, and $\delta_{27}, \delta_8, \delta_1 < \delta_8^D, \delta_1^D$ since there is less phase-space for $D\bar{D}$ than for PP. As said before, $SU(4)$-elasticity is not implemented: it would fix the χ_i to some large values and introduce relations between $\delta_{27}, \delta_8, \delta_1$ and δ_8^D, δ_1^D, leading to $\mathrm{Br}(B \to PP) \approx \mathrm{Br}\left(B \to D\bar{D}\right)$ (see (6)). Let us stress again that $SU(4)$ is used at no stage of the present analysis.

The factorization property of can now be used to separate the $D\bar{D} \rightleftharpoons PP$ rescattering effects from the $SU(3)$-elastic part. For the set of states (10), this is achieved by splitting the phases as (see (19))

$$\begin{aligned}&\sqrt{S_{\chi_8}}\left(\delta_{27}, \delta_8, \delta_8^D\right)\\ &= \underbrace{\sqrt{S_{\chi_8}}\left(\delta_{27}, \delta_8, \delta_8\right)}_{\substack{PP \rightleftharpoons PP\\ D\bar{D} \rightleftharpoons D\bar{D}}} \cdot \underbrace{\sqrt{S_{\chi_8}}\left(0, 0, \delta_8^D - \delta_8\right)}_{D\bar{D} \rightleftharpoons PP}\end{aligned} \tag{21}$$

The first factor does not depend on χ_8 and is related to the $SU(3)$-elastic rescattering matrix (13) as $\sqrt{S_{\chi_8}}(\delta_{27}, \delta_8, \delta_8) = \sqrt{S_{SU(3)}}(\delta_{27}, \delta_8, \delta_8)$, while the second factor contains all the effects of $D\bar{D} \rightleftharpoons PP$ mixing and becomes trivial if either $\delta_8^D = \delta_8$ or $\chi_8 = 0$. Proceeding similarly with the other multiplets, we now absorb the $D\bar{D} \rightleftharpoons PP$ part of the rescattering into effective quark diagrams:

$$\text{On-shell } c\bar{c} \text{ FSI: } \begin{cases} P_c^{\rm eff} = P_c - \beta,\\ PA_c^{\rm eff} = PA_c + \frac{2}{3}\beta + \alpha,\end{cases} \tag{22}$$

[1] Previous attempts to include $\bar{D}D$ ($\bar{D}D_s$) contributions to $B \to \pi\pi\,(\pi K)$ can be found in [20].

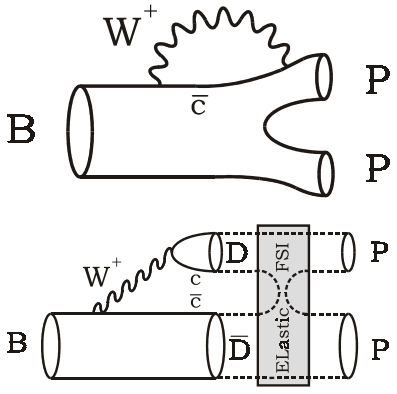

Fig. 3. The standard quark-level penguin amplitude P_c and the hadronic-level penguin-like $B \to \{D\bar{D}\} \to PP$ contribution

with

$$\alpha = \frac{1}{2\sqrt{3}}\left(1 - \mathrm{e}^{\mathrm{i}(\delta_1^D - \delta_1)}\right)\chi_1 T_D,$$
$$\beta = \sqrt{\frac{3}{5}}\left(1 - \mathrm{e}^{\mathrm{i}(\delta_8^D - \delta_8)}\right)\chi_8 T_D. \tag{23}$$

To reach these expressions, we have retained only the dominant T_D contribution to the $B \to D\overline{D}$ decay amplitudes (see Fig. 1) and the first order in χ_i (so that $PP \to D\overline{D} \to ... \to PP$ effects are neglected; see (19)). Importantly, all the other quark diagrams are unaffected by $D\bar{D} \rightleftharpoons PP$. Since the P_c and PA_c quark diagrams are precisely the ones involving the charm quark, we interpret (22) as a hadronic representation for on-shell intermediate $c\bar{c}$ quarks, as previously mentioned in [12] (see Fig. 3).

In general, because of renormalization of the penguin loop, it is desirable to use the unitarity of the CKM matrix to write ($\lambda_q \equiv V_{qb}^* V_{qd(s)}$)

$$\begin{aligned}\lambda_u P_u + \lambda_c P_c + \lambda_t P_t &= \lambda_u\left(P_u - P_c\right) + \lambda_t\left(P_t - P_c\right)\\ &\equiv \lambda_u\left(P_{u-c}\right) + \lambda_t\left(P_{t-c}\right).\end{aligned} \tag{24}$$

At the B-mass scale, we expect that P_{u-c} is small since $m_u, m_c \ll m_b$. Interestingly, when on-shell intermediate $c\bar{c}$ is treated at the hadronic level, the P_c short-distance absorptive part has to be discarded and to a large extent the cancellation between P_u and P_c is preserved. Therefore, one can expect the rough scaling of the dominant penguin contributions [9]

$$\begin{aligned} 1 &: T,\\ \mathcal{O}(\lambda) &: P_{t-c},\\ \mathcal{O}(\lambda^2) &: P_{t-c}^{\mathrm{EW}},\\ \mathcal{O}(\lambda^3) &: P_{C,t-c}^{\mathrm{EW}}, PA_{t-c},\end{aligned} \tag{25}$$

and $|X_{u-c}| < |X_{t-c}|$ with $X = P, PA, P^{\mathrm{EW}}, P_C^{\mathrm{EW}}$ to be valid. In the following, X_{u-c} will be neglected and the effects of intermediate charm will be accounted for by defining

$$\text{On-shell } c\bar{c} \text{ FSI: } \begin{cases} \lambda_t P_{t-c}^{\mathrm{eff}} = \lambda_t P_{t-c} - \lambda_c \beta,\\ \lambda_t PA_{t-c}^{\mathrm{eff}} = \lambda_t PA_{t-c} + \lambda_c\left(\frac{2}{3}\beta + \alpha\right).\end{cases} \tag{26}$$

Note that P_{t-c}^{eff} and PA_{t-c}^{eff} involve a combination of CP-conserving and CP-violating phases.

Our method for implementing intermediate on-shell charm has semi-inclusive features. To see this, note first that all the developments above can be repeated replacing $D\bar{D}$ by $D^*\bar{D}^*, D^{**}\bar{D}^{**}, ...$ Now, taking into account the effects on $B \to PP$ of rescatterings from all the charmed meson states amounts to the definitions (22) or (26) with α, β replaced by

$$\begin{aligned}\widetilde{\alpha} &= \frac{1}{2\sqrt{3}}F_1, \quad \widetilde{\beta} = \sqrt{\frac{3}{5}}F_8,\\ F_k &= \sum_{i=D,D^*,...}\left(1 - \mathrm{e}^{\mathrm{i}(\delta_k^i - \delta_k)}\right)\chi_k^i T_i,\end{aligned} \tag{27}$$

and this holds even if $D\bar{D} \rightleftharpoons D^*\bar{D}^*, ...$ rescatterings are present thanks to the factorization property (8) or (21). Finally, since in any case, the complex numbers $\widetilde{\alpha}$ and $\widetilde{\beta}$ can be parameterized as in (23), this change is irrelevant (except, of course, that χ and T_D can no longer be determined separately). In other words, as long as the χ_i are small (i.e. when the last term of (19) can be dropped), Watson's theorem implies that no matter the precise physics in the charmed sector, its impact on $B \to PP$ will always amount to a redefinition of the penguin amplitudes P_c and PA_c (or P_{t-c} and PA_{t-c}). In the following, for simplicity, we assume that $D\bar{D} \rightleftharpoons PP$ dominates so as to give estimations of χ_i. Finally, it is also straightforward to apply the formalism to charmonium modes $P\eta_c$ and/or $\eta_0\eta_c$ (see [21]), simply by substituting T_D by the C_{η_c} quark diagram contributing to $P\eta_c$ in β, and T_D by the C'_{η^c} contributing to $\eta_0\eta_c$ in α.

Let us conclude this section by a more technical comment. If we denote by $\bar{3}_c$ the $\bar{b}c.\bar{c}d$ or $\bar{b}c.\bar{c}s$ part of the weak Hamiltonian [10], P_c, PA_c and the definitions (22) are expressed in terms of $SU(3)$ reduced matrix elements as

$$\begin{cases} P_c = -\langle 8\,|\bar{3}_c|\,3\rangle\\ PA_c = \frac{2}{3}\langle 8\,|\bar{3}_c|\,3\rangle + \langle 1\,|\bar{3}_c|\,3\rangle\end{cases} \to$$
$$\begin{cases} \langle 8\,|\bar{3}_c|\,3\rangle^{\mathrm{eff}} = \langle 8\,|\bar{3}_c|\,3\rangle + \beta,\\ \langle 1\,|\bar{3}_c|\,3\rangle^{\mathrm{eff}} = \langle 1\,|\bar{3}_c|\,3\rangle + \alpha.\end{cases} \tag{28}$$

As expected, the $\alpha\,(\beta)$ term involving $\chi_1\,(\chi_8)$ contributes only to the reduced matrix element involving the 1 (8) final state, respectively.

2.3 Final parameterization

All the pieces can now be put together to construct the final parameterizations of $B \to PP$ decay amplitudes assuming enlarged $SU(3)$-elasticity. From the previous sections we have the following.

(1) All $PP \rightleftharpoons PP$ rescattering effects should be contained in $\sqrt{S}$, to preserve the scalings between quark diagram amplitudes, and will be treated assuming exact $SU(3)$ (see (15) and (16)).
(2) Intermediate charm can be treated at the hadronic level as $D\bar{D} \rightleftharpoons PP$ rescattering effects and absorbed into P_{t-c} and PA_{t-c} (see (26)).

The first point is important since it allows us to reduce the number of free parameters. Indeed, combining (16) and (25) with the CKM coefficients, it appears to be sufficient to consider only four topologies ($\lambda_q^{q'} \equiv V_{qb}^* V_{qq'}$)

$$\begin{aligned} &\Delta S = 0 : \lambda_u^d\, T, \quad \lambda_t^d\, P_{t-c}, \lambda_u^d\, C, \\ &\Delta S = 1 : \lambda_t^s P_{t-c}, \quad \lambda_u^s\, T, \lambda_t^s\, P_{t-c}^{\mathrm{EW}}, \end{aligned} \tag{29}$$

since in any case, $SU(3)$ breaking effects in the dominant T and P_{t-c} contributions should be greater than $\mathcal{O}\left(\lambda^2\right) \sim 4\%$.

Once PA is neglected, it seems justified to set also (see (26))

$$\frac{2}{3}\beta + \alpha = 0 \Leftrightarrow \begin{cases} \delta_1^D - \delta_1 = \delta_8^D - \delta_8, \\ \chi \equiv \chi_8 = -\frac{\sqrt{5}}{4}\chi_1, \end{cases} \tag{30}$$

since this combination describes rescatterings that proceeds through the vacuum ((30) may seem to imply a fine tuning between α and β, but this is equivalent to the usual assumption that PA_c is small, see (28)).

There remain eight free parameters

$$\begin{aligned} \text{QD amplitudes:} \quad & T, C, P_{t-c}, P_{t-c}^{\mathrm{EW}}, \\ SU(3)\text{ rescatterings:} \quad & \delta_{27} - \delta_1, \delta_8 - \delta_1, \\ \text{On-shell } c\bar{c} \text{ FSI:} \quad & \chi T_D, \delta_8^D - \delta_1. \end{aligned} \tag{31}$$

The expressions for decay amplitudes are collected in Appendix B, in which the definition (26) is used, δ_1 is set to zero and CKM coefficients are omitted. Also, the color-allowed electroweak penguin has to be introduced as $C \to C + P_{t-c}^{\mathrm{EW}}$ [9]. Decay amplitudes for $B \to D\bar{D}$, assuming that $D\bar{D}, PP \rightleftharpoons D^*\bar{D}^*, \ldots$ are negligible, are also given. In that case, measurements of $B \to D\bar{D}$ branchings can serve to determine both T_D and the strong phase $\delta_8 - \delta_1$ of $PP \rightleftharpoons PP$ rescattering. This fact originates in the coherence requirement (30), which implies (provided $\chi \neq 0$)

$$\begin{aligned} &\frac{\mathrm{Br}\left(B^0 \to D^+ D^-\right) \Gamma\left(B^0\right)}{\mathrm{Br}\left(B^+ \to D^+ \bar{D}^0\right) \Gamma\left(B^+\right)} \\ &= \frac{5 + 4\cos\left(\delta_8^D - \delta_1^D\right)}{9} = \frac{5 + 4\cos\left(\delta_8 - \delta_1\right)}{9}. \end{aligned} \tag{32}$$

3 Numerical examples

For our numerical examples, we consider only one source of rescattering: either $SU(3)$-elastic ones ($PP \rightleftharpoons PP$) or on-shell intermediate charm ($D\bar{D} \rightleftharpoons PP$). The sets of free parameters in each case are

$$\begin{array}{lcc} \text{Amplitudes:} & T, P_{t-c}, C, P_{t-c}^{\mathrm{EW}} & \\ & \swarrow \qquad\qquad & \searrow \\ \text{Rescattering:} & PP \rightleftharpoons PP & D\bar{D} \rightleftharpoons PP \\ & \delta_{27} - \delta_1, \delta_8 - \delta_1 & \chi T_D, \delta_8^D - \delta_1 \end{array} \tag{33}$$

with, in addition, the weak angle γ. To leading order, one can further neglect C and P_{t-c}^{EW}. Though the formalism allows for general analyses, the precision of the experimental data is not yet sufficient for meaningful combined analyses.

For each fit, we give the values of the parameters in the text, while the corresponding values for branchings (Table 6), A_{CP} (Table 7) and $S_{f\bar{f}}$ (Table 8) are in Appendix C, along with the details of our fitting procedure.

Table 1. T, P_{t-c}, $SU(3)$-elasticity

γ	60°	80°	100°
$\chi^2_{\min}$	18.3	16.3	17.7
T	0.65	0.70	0.76
P_{t-c}	0.11	0.11	0.10
$\delta_8 - \delta_1$	47°	52°	62°
$\delta_{27} - \delta_1$	100°	98°	101°

3.1 $SU(3)$-elasticity (no $D\bar{D} \rightleftharpoons PP$)

For the first example, we take the T and P_{t-c} amplitudes and $\delta_8 - \delta_1$, $\delta_{27} - \delta_1$ strong phases (so we set $\chi = 0$). For various (fixed) values of the weak angle γ we find the results of Table 1. Quark diagram amplitudes given in the table are dimensionless and produce B^0 branchings.

Under this $SU(3)$-elastic parameterization, the $B \to \pi K$ branchings are dominated by the P_{t-c} penguin amplitude and verify

$$\begin{aligned} &\mathrm{Br}\left(\pi^0 K^+\right) : \mathrm{Br}\left(\pi^+ K^0\right) : \mathrm{Br}\left(\pi^0 K^0\right) : \mathrm{Br}\left(\pi^- K^+\right) \\ &\quad \approx 1/2 : 1 : 1/2 : 1, \end{aligned} \tag{34}$$

while the pattern of direct CP-asymmetries is [12]

$$A_{\pi^0 K^+} : A_{\pi^+ K^0} : A_{\pi^0 K^0} : A_{\pi^- K^+} \approx 2 : -\frac{1}{2} : -\frac{3}{2} : 1, \tag{35}$$

no matter what the strong phases are.

As already found in [14], if the current CP-asymmetry measurement central values are to be trusted, they require large $PP \rightleftharpoons PP$ phases. Then, in the $B \to \pi\pi$ sector, dominated by T, large rescatterings occur and the $\pi^0\pi^0$ mode is fed from $B \to \{\pi^+\pi^-\}$. The resulting pattern is close to

$$\mathrm{Br}\left(\pi^+\pi^0\right) : \mathrm{Br}\left(\pi^+\pi^-\right) : \mathrm{Br}\left(\pi^0\pi^0\right) \approx 1 : 1 : 1/2. \tag{36}$$

Typically, $\mathrm{Br}\left(B^0 \to \pi^0\pi^0\right) > 1.5 \times 10^{-6}$ under $SU(3)$-elasticity. For $\pi^+\pi^-$ time-dependent asymmetry, both

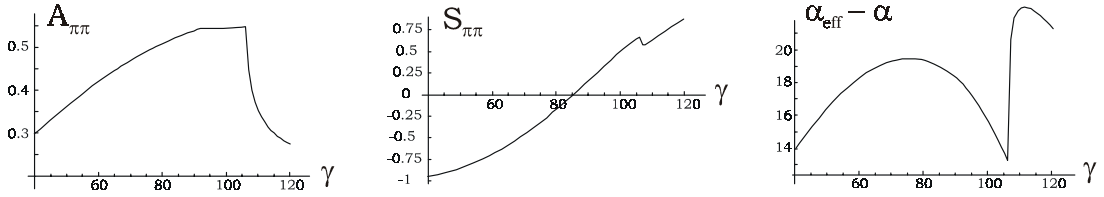

Fig. 4. Fit result for $A_{\pi^+\pi^-}, S_{\pi^+\pi^-}$ and $\alpha_{\rm eff}$ under $SU(3)$-elasticity

Table 2. $T, P_{t-c}, C, P_{t-c}^{\rm EW}$, $SU(3)$-elasticity

γ	60°	80°	100°
$\chi^2_{\rm min}$	10.1	10.5	15.4
T	0.60	0.66	0.67
C	0.21	0.17	0.17
P_{t-c}	0.11	0.11	0.10
$P_{t-c}^{\rm EW}$	0.011	0.008	0.005
$\delta_8 - \delta_1$	53°	57°	32°
$\delta_{27} - \delta_1$	88°	89°	59°

$A_{\pi^+\pi^-}$ and $S_{\pi^+\pi^-}$ are found to be compatible with the current experimental data (see Appendix C and see Fig. 4).

$A_{\pi^+\pi^-}$ is not very sensitive to γ and stays in the range 0.3 to 0.5. On the other hand, $S_{\pi^+\pi^-}$ varies much, and it appears that the present Belle measurement exclude $\gamma > 90^\circ$ to 3σ. However, the dependence of $S_{\pi^+\pi^-}$ on γ is rather trivial. Defining the parameter $\alpha_{\rm eff}$ by

$$S_{\pi^+\pi^-} = \sqrt{1 - A^2_{\pi^+\pi^-}}\,\sin\left(2\alpha_{\rm eff}\right), \tag{37}$$

such that $\alpha_{\rm eff} = \alpha \equiv \pi - \beta - \gamma$ if only T contributes to $B^0 \to \pi^+\pi^-$, the last graph shows that the deviation $\alpha_{\rm eff} - \alpha$ stays small compared to γ.

Finally, for $B \to K\bar{K}$, no clear pattern emerges. However, one can note that because of large rescatterings from $B \to \{\pi^+\pi^-\}$, the $B^+ \to K^+K^-$ branching is saturating its present experimental upper bound. Also, the $B^+ \to K^+\bar{K}^0$ and $B^0 \to K^0\bar{K}^0$ direct CP-asymmetries tend to be sizable, between -1 and -0.5.

Just for illustration, if we now introduce the subleading C and $P_{t-c}^{\rm EW}$ topologies; the best-fit values are as in Table 2. The most noticeable feature is a reduction of the strong phases, at the cost of a quite large C amplitude, and a significant decrease in $\chi^2_{\rm min}$.

To within 20%, the introduction of the additional quark diagram amplitudes does not modify the patterns described above. For example, the ratios of CP-asymmetries in the πK sector are now

$$\begin{aligned} &A_{\pi^0K^+} : A_{\pi^+K^0} : A_{\pi^0K^0} : A_{\pi^-K^+} \\ &= 2 + \frac{8}{5}\kappa_{-1} : -\frac{1}{2} + \frac{3}{5}\kappa_{2/3} : -\frac{3}{2} + 3\kappa_0 : 1, \end{aligned} \tag{38}$$

with, to leading order in $|\lambda_u^s|\,T/|\lambda_t^s|\,P_{t-c}$ and $P_{t-c}^{\rm EW}/P_{t-c}$,

$$\kappa_\alpha = \cos\gamma \frac{|\lambda_u^s|\,T}{|\lambda_t^s|\,P_{t-c}}$$

Table 3. Measurements of $A_{\pi^-K^+}$ by Belle, BaBar and $A_{\pi^0K^+}$ by Belle

	Belle
$A_{\pi^-K^+}$	$-0.088 \pm 0.035 \pm 0.018$ [4]
$A_{\pi^0K^+}$	$0.23 \pm 0.11^{+0.01}_{-0.04}$ [2]

	BaBar
$A_{\pi^-K^+}$	$-0.107 \pm 0.041 \pm 0.013$ [4]
$A_{\pi^0K^+}$	$-0.09 \pm 0.09 \pm 0.01$ [3]

$$\times \left(\cos\left(\delta_8 - \delta_{27}\right)\left(1 + \frac{C}{T}\right) + \alpha\left(1 - \frac{3C}{2T}\right)\right) \tag{39}$$
$$-\frac{P_{t-c}^{\rm EW}}{P_{t-c}}\left(\cos\left(\delta_8 - \delta_{27}\right) - \frac{\alpha}{4}\left(1 + \frac{5C}{C+T}\right)\right).$$

For the range of parameter values in Table 2, these corrections are of at most 15% (see Table 7).

To close this section, it should be noted that the $SU(3)$-elastic constraint $A_{\pi^0K^+} = 2A_{\pi^-K^+}$, though consistent, is not favored by the present measurements of $A_{\pi^-K^+}$ by Belle, BaBar and $A_{\pi^0K^+}$ by Belle; see Table 3. Further, as shown in [12], this constraint is the same under $SU(2)$-elasticity. More precise measurements are necessary to draw any conclusion on the relevance of $SU(N)$-elastic rescatterings for $B \to PP$.

3.2 On-shell $c\bar{c}$ rescattering (no $PP \rightleftharpoons PP$)

For our second example, we take again the T and P_{t-c} amplitudes, but $\delta_8^D - \delta_8$ as the only strong phase. In addition, we have the T_D amplitude and the mixing angle χ. As a first step, since it is always the combination (χT_D) which appears in $B \to PP$ decays, we can use the measurements [22] $\mathrm{Br}\left(B^0 \to D^- D_s^+\right) = (0.8 \pm 0.3)\,\%$ and $\mathrm{Br}\left(B^+ \to \bar{D}^0 D_s^+\right) = (1.3 \pm 0.4)\,\%$ to fix $T_D = 2.43$ which gives

$$\mathrm{Br}^{\rm th}\left(B^0 \to D^- D_s^+\right) = \mathrm{Br}^{\rm th}\left(B^+ \to \bar{D}^0 D_s^+\right) = 0.98\%. \tag{40}$$

For various weak angles γ we find the results of Table 4. Note that the fitting procedure is delicate because, to a large extent, P_{t-c} and χT_D compete against each other (see (26)) and the $\chi^2_{\rm min}$ function is rather flat. The above results are those for which both χ and $\delta_8^D - \delta_8$ are simultaneously small.

The $B \to \pi K$ branchings are now dominated by both P_{t-c} and $B \to \left\{\bar{D}D_s\right\} \to \pi K$ contributions, and

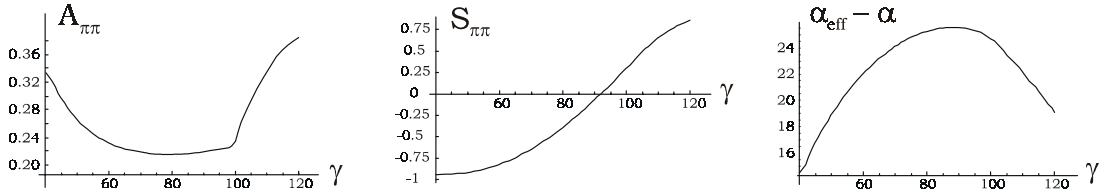

Fig. 5. Fit result for $A_{\pi^+\pi^-}, S_{\pi^+\pi^-}$ and $\alpha_{\rm eff}$ under on-shell $c\bar{c}$ rescattering

Table 4. T, P_{t-c}, on-shell $c\bar{c}$

γ	60°	80°	100°
$\chi^2_{\rm min}$	40	32	26
T	0.50	0.57	0.66
P_{t-c}	0.09	0.10	0.10
χ	3.3°	2.7°	2.6°
$\delta_8^D - \delta_8$	25°	21°	20°

since these effects behave like a "hadronic" penguin, see (26), the pattern (34) is not altered. Concerning CP-asymmetries, we find the pattern

$$A_{\pi^0K^+} : A_{\pi^+K^0} : A_{\pi^0K^0} : A_{\pi^-K^+} \approx 1 : -\frac{P_{t-c}}{T} : -\frac{P_{t-c}}{T} : 1. \tag{41}$$

Interestingly, some ratios of CP-asymmetries directly give the value of P_{t-c}/T. These asymmetries are generated through the interference of T, P_{t-c} with $B \to \{\bar{D}D_s\} \to \pi K$, and require only one strong phase $\delta_8^D - \delta_8$ of less than about 25° (generated by the mismatch between $PP \rightleftharpoons PP$ and $D\bar{D} \rightleftharpoons D\bar{D}$; see (20)).

In the $B \to \pi\pi$ sector, the fit is not very good (the large $\chi^2_{\rm min}$ is essentially generated by the $\pi^0\pi^0$ and $\pi^0\pi^+$ modes). Indeed, the $B \to \{\bar{D}D\} \to \pi\pi$ effects are Cabibbo-suppressed, and since there is no averaging from $PP \rightleftharpoons PP$ strong phases, the decay branchings keep their bare scalings in terms of dominant T (see Appendix B):

$$\mathrm{Br}\left(\pi^+\pi^0\right) : \mathrm{Br}\left(\pi^+\pi^-\right) : \mathrm{Br}\left(\pi^0\pi^0\right) \approx 1/2 : 1 : 0, \tag{42}$$

which is rather far from current measurements (but not yet ruled out; see Table 6, Appendix C). Typically, $\mathrm{Br}\left(B \to \pi^0\pi^0\right) < 10^{-6}$ without $PP \rightleftharpoons PP$ strong phases (and assuming $C/T \sim \mathcal{O}(\lambda)$ or smaller). Finally, $A_{\pi^+\pi^-}$ is found to be a bit smaller (in the range 0.2 to 0.4), while $S_{\pi^+\pi^-}$ behaves roughly as in the $SU(3)$-elastic case (see Fig. 5).

Note, however, that $\alpha_{\rm eff} \neq \alpha$ is now due to both $B \to \{D\bar{D}\} \to \pi\pi$ and P_{t-c}, and, therefore, that P_{t-c} does not imply $\alpha_{\rm eff} = \alpha$ (this is obvious from (26)).

For $B \to K\bar{K}$, the branchings are similar than in the $SU(3)$-elastic case except for $B^0 \to K^+K^-$ which is exactly zero (no rescattering from $B \to \{\pi^+\pi^-\}$ and no $B \to \{D\bar{D}\} \to K^+K^-$ because of (30)). The $B^+ \to K^+\bar{K}^0$ and $B^0 \to K^0\bar{K}^0$ direct CP-asymmetries tend to be much smaller (between 0 and -0.3), and in addition verifies

$$A_{K^+\bar{K}^0} : A_{K^0\bar{K}^0} : A_{\pi^0\pi^0} = 1 : 1 : 1. \tag{43}$$

Table 5. $T, P_{t-c}, C, P^{\rm EW}_{t-c}$, on-shell $c\bar{c}$

γ	60°	80°	100°
$\chi^2_{\rm min}$	18	14	12
T	0.49	0.55	0.62
C	0.24	0.20	0.23
P_{t-c}	0.09	0.09	0.09
$P^{\rm EW}_{t-c}$	0.011	0.006	0.004
χ	3.5°	2.6°	4.7°
$\delta_8^D - \delta_8$	26°	26°	15°

If we now include the subleading C and $P^{\rm EW}_{t-c}$, the best fit procedure produces a large C amplitude to match the observed pattern of $B \to \pi\pi$ branchings (we have restricted C/T to be at most 1/2); see Table 5. The pattern of $B \to \pi K$ direct CP-asymmetries is much affected by such a large C amplitude

$$\begin{aligned} &A_{\pi^0K^+} : A_{\pi^+K^0} : A_{\pi^0K^0} : A_{\pi^-K^+} \\ &= 1 + \frac{C}{T} + \frac{CP_{t-c}}{T^2} : -\frac{P_{t-c}}{T} : -\frac{P_{t-c}+C}{T} - \frac{CP_{t-c}}{T^2} : 1, \end{aligned} \tag{44}$$

while corrections due to $P^{\rm EW}_{t-c}$ are subleading. Notice, however, that for the range of values in Table 5, this pattern is still different from the $SU(3)$-elastic one (35). Finally, the pattern (43) survives only partially: while $A_{K^+\bar{K}^0}$ and $A_{K^0\bar{K}^0}$ remain exactly equal (no C or $P^{\rm EW}_{t-c}$ contribution), $A_{\pi^0\pi^0}$ is dominated by C and varies much.

To close this section, let us make a few comments. First, note that phenomenologically speaking, $P_{t-c}/T = 0$ is not yet ruled out by experiment once the penguin-like rescattering effects $B \to \{D\bar{D}\} \to PP$ are allowed. Indeed, the $B \to K\pi$ branchings could be dominated by the $B \to \{D_s\bar{D}\} \to \pi K$ contributions, while both $B \to \pi K$ and $B \to \pi^+\pi^-$ direct CP-asymmetries could be generated by interference of $B \to \{D\bar{D}\} \to PP$ contributions with T. In other words, assuming that $D\bar{D} \rightleftharpoons PP$ is the dominant rescattering process, the current data require $\left|P^{\rm eff}_{t-c}/T\right| \neq 0$ with $P^{\rm eff}_{t-c}$ given in (26), but do not say anything yet about the relative strength of the quark-level penguin P_{t-c} versus its hadronic-level counterpart $B \to \{D\bar{D}\} \to PP$. Now, theoretically, from short-distance analyses there is good reasons to expect $P_{t-c}/T \neq 0$, and we hope that the phenomenological patterns of CP-asymmetries described above will help in extracting it from the data.

Second, under exact flavor $SU(3)$, it appears that consistency with $B \to \pi K$ direct CP-asymmetry measure-

ments restricts $A_{\pi\pi}$ to be smaller than ~ 0.5. This statement is independent of the precise physics in the charmed meson sector. Except for the values quoted for χ, the results of the fits are equally valid when the intermediate charmed meson state is $D\bar{D}$, $D^*\bar{D}^*, ...$ or a charmonium state like $P\eta_c$ [21], or also combinations of them. Further, the rescattering between these states is irrelevant for $B \to PP$. Note also that abandoning the coherence requirement (30) does not lead to larger $A_{\pi\pi}$, even if $PA_c^{\rm eff} = PA_c + 2/3\beta + \alpha \approx 2/3\beta + \alpha$ (see (22)) contributes to $B^0 \to \pi^+\pi^-$ and not to $B \to \pi K$, because $PA_c^{\rm eff}$ also contributes to $B^0 \to K^+K^-$ and therefore cannot be large.

Finally, it should be noted that many relations between B^0, B^+ direct CP-asymmetry and B_S ones exist:

$$A_{B_S\to\pi^+K^-} = A_{B^0\to\pi^+\pi^-},$$
$$A_{B_S\to K^0\bar{K}^0} = A_{B^+\to\pi^+K^0},$$
$$A_{B_S\to\pi^0\bar{K}^0} = A_{B^0\to\pi^0\pi^0},$$
$$A_{B_S\to K^+K^-} = A_{B^0\to\pi^-K^+}.$$

All these relations are unaffected by C or $P_{t-c}^{\rm EW}$ contributions and specific to the dominant on-shell $c\bar{c}$ rescattering source (no $PP \rightleftharpoons PP$ rescatterings).

4 Conclusions

The B to two charmless pseudoscalar decay processes are analyzed assuming exact $SU(3)$ for the amplitudes and rescatterings. The basic tool is Watson's theorem for hadronic final state interactions, which allows for a factorization of rescattering effects from bare decay amplitudes. In addition, the various FSI processes can also be factorized and treated separately. In the present work, we assume $SU(3)$-elasticity for the $PP \rightleftharpoons PP$ part of the rescatterings, while $D\bar{D} \rightleftharpoons PP$ elastic rescatterings are shown to amount to the redefinition of the penguin amplitude as

$$\lambda_t P_{t-c}^{\rm eff} = \lambda_t P_{t-c} - \lambda_c \sqrt{\frac{3}{5}} \left(1 - {\rm e}^{{\rm i}(\delta_8^D - \delta_8)}\right) \chi T_D, \quad (45)$$

where T_D is the tree diagram contributing to $B \to D\bar{D}$ and χ the small mixing parameter governing the $D\bar{D}$ pollution of $B \to PP$ (this parameter is not fixed by $SU(3)$, and must be small because of (6)). Importantly, the redefinition (45) also applies when the intermediate charmed meson state is $D^*\bar{D}^*, D^{**}\bar{D}^{**}, P\eta_c, ...$, or any combination of them, and therefore (45) can be seen as a hadronic representation for on-shell intermediate $c\bar{c}$.

Also, it should be clear that once the various rescattering effects can be treated separately, different theoretical tools can be combined. This is well illustrated by (45): if one has a definite computation scheme for $P_{t-c}^{\rm eff}$ accounting for (elastic or inelastic) intermediate on-shell $c\bar{c}$ but suspects non-negligible elastic long-distance $PP \rightleftharpoons PP$ rescatterings, the present formalism permits the combination of the two. In other words, it is perfectly consistent to account for $SU(N)$-elastic long-distance rescatterings by acting with the corresponding $\sqrt{S_{SU(N)}}$ on effective quark diagram amplitudes already containing various rescattering effects, like those produced by QCD-based approaches.

In our phenomenological approach, many amplitudes can be safely ignored and we are left with the set of free parameters (31), with, in addition, the weak angle γ. To further restrict the number of free parameters, one rescattering source is assumed dominant: either $SU(3)$-elasticity ($PP \rightleftharpoons PP$) or on-shell $c\bar{c}$ ($D\bar{D} \rightleftharpoons PP$). The most prominent features of each fit are as follows.
(1) *SU(3)-elasticity:* The $B \to \pi K$ direct CP-asymmetries tend to require large strong phases. This is nice for $B \to \pi\pi$ (see (36)) but may be problematic for $B \to KK$ (those modes are predicted to be close to their present experimental upper bounds). Also, it should be noted that the $SU(3)$-elastic pattern of $B \to \pi K$ direct CP-asymmetries (35) is rather insensitive to subleading quark diagram amplitudes (C and $P_{t-c}^{\rm EW}$), and is not in good agreement with present measurements (though the discrepancy is not yet significant).
(2) *On-shell $c\bar{c}$*: A single strong phase difference ($\delta_8^D - \delta_8$) of around 25° is sufficient to produce the required asymmetries in the πK and $\pi\pi$ sectors. This strong phase difference is generated by the mismatch between $PP \rightleftharpoons PP$ and $D\bar{D} \rightleftharpoons D\bar{D}$ elastic rescattering channels. Such a small strong phase is nice from the point of view of Regge computations [15] and from the naive expectation for two particle flying apart with large momentum [16], but also with the $SU(2)$-elastic isospin analysis of $B \to D\pi$ [23]. Compared with the $SU(3)$-elastic case, the fit is not very good in the $B \to \pi\pi$ sector (no rescattering from $B \to \pi^+\pi^-$ leads to the approximate pattern (42)), but better for $B \to \pi K$ direct CP-asymmetries (the pattern (41) is favored by current measurements).

Combining both sources of rescattering would certainly improve the quality of the fit as more free parameters are available. For example, the difficulty of the on-shell $c\bar{c}$ fit in the $B \to \pi\pi$ sector is reduced by including a small amount of $PP \rightleftharpoons PP$ effects (like $\delta_{27} - \delta_8 \approx 20°$). More precise measurements are necessary to pursue the analysis in that direction.

Acknowledgements. Many thanks are due to J.-M. Gérard, J. Pestieau and J. Weyers for their helpful comments. This work was supported by the Federal Office for Scientific, Technical and Cultural Affairs through the Interuniversity Attraction Pole P5/27, and by the Institut Interuniversitaire des Sciences Nucléaires.

A Rescattering matrix for $T_3 = Y = 0$ states

This appendix presents the construction of the enlarged $SU(3)$ rescattering matrix for the $T_3 = Y = 0$ states. We start with

$$\begin{pmatrix} |27,2,0,0\rangle \\ |27,1,0,0\rangle \\ |27,0,0,0\rangle \\ |8,1,0,0\rangle \\ |8,0,0,0\rangle \\ |1,0,0,0\rangle \\ |8_D,1,0,0\rangle \\ |8_D,0,0,0\rangle \\ |1_D,0,0,0\rangle \end{pmatrix} = \underbrace{\begin{pmatrix} & & & & & & 0 & 0 & 0 \\ & & & & & & 0 & 0 & 0 \\ & & & O^{PP}_{SU(3)} & & & 0 & 0 & 0 \\ & & & & & & 0 & 0 & 0 \\ & & & & & & 0 & 0 & 0 \\ & & & & & & 0 & 0 & 0 \\ 0 & 0 & 0 & 0 & 0 & 0 & & & \\ 0 & 0 & 0 & 0 & 0 & 0 & & O^{D\bar{D}}_{SU(3)} & \\ 0 & 0 & 0 & 0 & 0 & 0 & & & \end{pmatrix}}_{O_{SU(3)}} \begin{pmatrix} \{K^+K^-\} \\ \left\{K^0\overline{K}^0\right\} \\ \{\eta_8\eta_8\} \\ \left\{\pi^0\eta_8\right\} \\ \{\pi^+\pi^-\} \\ \left\{\pi^0\pi^0\right\} \\ \{D^+D^-\} \\ \left\{D^0\bar{D}^0\right\} \\ \{D_s^+D_s^-\} \end{pmatrix},$$

where (entries are written according to $x = \text{sign}\,(x)\sqrt{|x|}$)

$$O^{PP}_{SU(3)} = \begin{pmatrix} 0 & 0 & 0 & 0 & -1/3 & 2/3 \\ -1/5 & 1/5 & 0 & 3/5 & 0 & 0 \\ -3/20 & -3/20 & 27/40 & 0 & 1/60 & 1/120 \\ 3/10 & -3/10 & 0 & 2/5 & 0 & 0 \\ -1/10 & -1/10 & -1/5 & 0 & 2/5 & 1/5 \\ -1/4 & -1/4 & -1/8 & 0 & -1/4 & -1/8 \end{pmatrix},$$

$$O^{D\bar{D}}_{SU(3)} = \begin{pmatrix} 1/2 & 1/2 & 0 \\ -1/6 & 1/6 & 2/3 \\ -1/3 & 1/3 & -1/3 \end{pmatrix}$$

To introduce rescattering between $D\bar{D}$ and PP, it suffices to mix $|8,1,0,0\rangle$ with $|8_D,1,0,0\rangle$, $|8,0,0,0\rangle$ with $|8_D,0,0,0\rangle$ and $|1,0,0,0\rangle$ with $|1_D,0,0,0\rangle$ by defining

$$O_\chi = \begin{pmatrix} 1\,0\,0 & 0 & 0 & 0 & 0 & 0 & 0 \\ 0\,1\,0 & 0 & 0 & 0 & 0 & 0 & 0 \\ 0\,0\,1 & 0 & 0 & 0 & 0 & 0 & 0 \\ 0\,0\,0 & \cos\chi_8 & 0 & 0 & \sin\chi_8 & 0 & 0 \\ 0\,0\,0 & 0 & \cos\chi_8 & 0 & 0 & \sin\chi_8 & 0 \\ 0\,0\,0 & 0 & 0 & \cos\chi_1 & 0 & 0 & \sin\chi_1 \\ 0\,0\,0 & -\sin\chi_8 & 0 & 0 & \cos\chi_8 & 0 & 0 \\ 0\,0\,0 & 0 & -\sin\chi_8 & 0 & 0 & \cos\chi_8 & 0 \\ 0\,0\,0 & 0 & 0 & -\sin\chi_1 & 0 & 0 & \cos\chi_1 \end{pmatrix}.$$

Finally, the rescattering matrix is found as $\sqrt{S_\chi} = O^{\text{t}}_{SU(3)}.O^{\text{t}}_\chi.\sqrt{S_{\text{diag}}}.O_\chi.O_{SU(3)}$, with, when the χ_i are small,

$$S_{\text{diag}} = \text{diag}\left(\text{e}^{2\text{i}\delta_{27}}, \text{e}^{2\text{i}\delta_{27}}, \text{e}^{2\text{i}\delta_{27}}, \text{e}^{2\text{i}\delta_8}, \text{e}^{2\text{i}\delta_8}, \text{e}^{2\text{i}\delta_1}, \text{e}^{2\text{i}\delta_8^D}, \text{e}^{2\text{i}\delta_8^D}, \text{e}^{2\text{i}\delta_1^D}\right).$$

B Decay amplitude expressions

The $B \to PP$ decay amplitudes, under the approximations discussed in the text, are

$$\begin{aligned}
&\mathcal{A}(B^+ \to K^+\bar{K}^0) \\
&= \frac{\text{e}^{\text{i}\delta_8} - \text{e}^{\text{i}\delta_{27}}}{5}(T+C) + \text{e}^{\text{i}\delta_8}P^{\text{eff}}_{t-c}, \\
&\mathcal{A}(B^0 \to K^+K^-) \\
&= \frac{5\left(1-\text{e}^{\text{i}\delta_8}\right) + \left(\text{e}^{\text{i}\delta_8} - \text{e}^{\text{i}\delta_{27}}\right)}{20}T \\
&- \frac{5\left(1-\text{e}^{\text{i}\delta_8}\right) - 3\left(\text{e}^{\text{i}\delta_8} - \text{e}^{\text{i}\delta_{27}}\right)}{60}C + \frac{2\left(1-\text{e}^{\text{i}\delta_8}\right)}{3}P^{\text{eff}}_{t-c}, \\
&\mathcal{A}(B^0 \to K^0\bar{K}^0) \\
&= \frac{5\left(1-\text{e}^{\text{i}\delta_8}\right) + \left(\text{e}^{\text{i}\delta_8} - \text{e}^{\text{i}\delta_{27}}\right)}{20}T \\
&- \frac{5\left(1-\text{e}^{\text{i}\delta_8}\right) - 3\left(\text{e}^{\text{i}\delta_8} - \text{e}^{\text{i}\delta_{27}}\right)}{60}C + \frac{2+\text{e}^{\text{i}\delta_8}}{3}P^{\text{eff}}_{t-c}, \\
&\mathcal{A}(B^+ \to \pi^+\pi^0) = \frac{\text{e}^{\text{i}\delta_{27}}}{\sqrt{2}}(T+C), \\
&\mathcal{A}(B^0 \to \pi^+\pi^-) \\
&= \frac{5+8\text{e}^{\text{i}\delta_8} + 7\text{e}^{\text{i}\delta_{27}}}{20}T \\
&- \frac{5\left(1-\text{e}^{\text{i}\delta_8}\right) + 21\left(\text{e}^{\text{i}\delta_8} - \text{e}^{\text{i}\delta_{27}}\right)}{60}C + \frac{2+\text{e}^{\text{i}\delta_8}}{3}P^{\text{eff}}_{t-c}, \\
&\mathcal{A}(B^0 \to \pi^0\pi^0) \\
&= \frac{5\left(1-\text{e}^{\text{i}\delta_8}\right) + 13\left(\text{e}^{\text{i}\delta_8} - \text{e}^{\text{i}\delta_{27}}\right)}{20\sqrt{2}}T \\
&- \frac{5+16\text{e}^{\text{i}\delta_8} + 39\text{e}^{\text{i}\delta_{27}}}{60\sqrt{2}}C + \frac{2+\text{e}^{\text{i}\delta_8}}{3\sqrt{2}}P^{\text{eff}}_{t-c}, \\
&\mathcal{A}(B^+ \to K^+\pi^0) \\
&= \frac{\text{e}^{\text{i}\delta_8} + 4\text{e}^{\text{i}\delta_{27}}}{5\sqrt{2}}(T+C) + \frac{\text{e}^{\text{i}\delta_8}}{\sqrt{2}}P^{\text{eff}}_{t-c}, \\
&\mathcal{A}(B^+ \to K^0\pi^+) \\
&= \frac{\text{e}^{\text{i}\delta_8} - \text{e}^{\text{i}\delta_{27}}}{5}(T+C) + \text{e}^{\text{i}\delta_8}P^{\text{eff}}_{t-c}, \\
&\mathcal{A}(B^0 \to K^+\pi^-) \\
&= \frac{3\text{e}^{\text{i}\delta_8} + 2\text{e}^{\text{i}\delta_{27}}}{5}T + \frac{2\left(\text{e}^{\text{i}\delta_{27}} - \text{e}^{\text{i}\delta_8}\right)}{5}C + \text{e}^{\text{i}\delta_8}P^{\text{eff}}_{t-c}, \\
&\mathcal{A}(B^0 \to K^0\pi^0) \\
&= \frac{3\left(\text{e}^{\text{i}\delta_{27}} - \text{e}^{\text{i}\delta_8}\right)}{5\sqrt{2}}T + \frac{2\text{e}^{\text{i}\delta_8} + 3\text{e}^{\text{i}\delta_{27}}}{5\sqrt{2}}C - \frac{\text{e}^{\text{i}\delta_8}}{\sqrt{2}}P^{\text{eff}}_{t-c}, \\
&\mathcal{A}\left(B^+ \to \pi^+\eta_8\right)
\end{aligned}$$

Table 6. Fit results for charge-average branching fractions

Branching ($\times 10^{-6}$)			$SU(3)$-elastic				On-shell $c\bar{c}$			
			Table 1		Table 2		Table 3		Table 4	
$\Delta S = 0$		Exp.	60°	90°	60°	90°	60°	90°	60°	90°
	$\overline{K^0}\eta_8$	–	0.43	0.37	0.31	0.42	0.13	0.18	0.22	0.45
B_S	$\overline{K^0}\pi^0$	–	1.29	1.10	0.93	1.26	0.38	0.53	0.65	1.35
	$K^-\pi^+$	–	5.91	5.78	5.72	4.61	4.77	4.72	4.55	4.24
	$\pi^+\eta_8$	$[4.0 \pm 0.9]$	1.59	1.38	2.41	1.72	1.42	1.17	2.31	1.93
B^+	$\overline{K^0}K^+$	<1.3	1.09	1.28	1.01	1.28	0.88	1.21	0.89	1.18
	$\pi^+\pi^0$	5.3 ± 0.8	3.48	4.42	5.43	5.67	2.07	3.10	4.34	5.86
	K^+K^-	<0.6	0.60	0.60	0.60	0.15	0	0	0	0
	$K^0\overline{K^0}$	<1.6	1.02	1.31	0.93	1.14	0.81	1.11	0.82	1.08
B^0	$\eta_8\eta_8$	–	0.17	0.25	0.12	0.09	0.05	0.06	0.11	0.09
	$\pi^0\eta_8$	$[<2.9]$	0.26	0.38	0.26	0.38	0.27	0.37	0.27	0.36
	$\pi^+\pi^-$	4.6 ± 0.4	4.82	4.79	4.58	4.53	5.03	4.98	4.80	4.47
	$\pi^0\pi^0$	1.92 ± 0.44	2.12	1.70	1.77	1.57	0.41	0.56	0.68	1.43
$\Delta S = 1$		Exp.	60°	90°	60°	90°	60°	90°	60°	90°
	$K^0\eta_8$	$[2.4 \pm 0.9]$	3.33	3.17	2.94	2.82	3.37	3.17	2.92	2.86
B^0	$K^0\pi^0$	11.2 ± 1.4	9.98	9.51	8.81	8.45	10.1	9.51	8.75	8.57
	$K^+\pi^-$	18.2 ± 0.8	18.6	19.2	18.3	19.0	18.6	19.2	18.5	19.1
	$K^+\eta_8$	$[3.1 \pm 0.7]$	4.02	3.52	3.68	3.20	4.02	3.51	3.50	3.20
B^+	$K^+\pi^0$	12.8 ± 1.1	10.3	10.4	11.7	11.7	10.1	10.4	11.6	11.6
	$K^0\pi^+$	20.6 ± 1.4	22.0	20.6	22.3	20.7	22.0	20.6	21.8	20.5
	K^+K^-	–	15.5	14.7	14.2	16.9	17.6	18.2	17.6	18.1
	$K^0\overline{K^0}$	–	16.6	14.5	15.9	17.0	19.2	18.0	19.0	17.9
B_S	$\eta_8\eta_8$	–	14.1	12.5	12.9	14.2	17.0	16.0	15.8	15.2
	$\pi^0\eta_8$	–	0.03	0.02	0.05	0.04	0	0	0.05	0.03
	$\pi^+\pi^-$	–	5.19	6.95	6.55	1.95	0	0	0	0
	$\pi^0\pi^0$	–	2.59	3.48	3.28	0.97	0	0	0	0

$$= \frac{2e^{i\delta_8} + 3e^{i\delta_{27}}}{5\sqrt{6}}(T + C) + \frac{2e^{i\delta_8}}{\sqrt{6}}P^{\text{eff}}_{t-c},$$

$$\mathcal{A}\left(B^0 \to \pi^0\eta_8\right) = -\frac{e^{i\delta_8}}{\sqrt{3}}P^{\text{eff}}_{t-c},$$

$$\mathcal{A}\left(B^+ \to K^+\eta_8\right)$$

$$= -\frac{e^{i\delta_8} - 6e^{i\delta_{27}}}{5\sqrt{6}}(T + C) - \frac{e^{i\delta_8}}{\sqrt{6}}P^{\text{eff}}_{t-c},$$

$$\mathcal{A}\left(B^0 \to K^0\eta_8\right)$$

$$= \frac{3\left(e^{i\delta_{27}} - e^{i\delta_8}\right)}{5\sqrt{6}}T + \frac{2e^{i\delta_8} + 3e^{i\delta_{27}}}{5\sqrt{6}}C - \frac{e^{i\delta_8}}{\sqrt{6}}P^{\text{eff}}_{t-c},$$

$$\mathcal{A}\left(B^0 \to \eta_8\eta_8\right)$$

$$= \frac{5\left(1 - e^{i\delta_8}\right) - 3\left(e^{i\delta_8} - e^{i\delta_{27}}\right)}{20\sqrt{2}}T$$

$$- \frac{5 - 16e^{i\delta_8} - 9e^{i\delta_{27}}}{60\sqrt{2}}C + \frac{2 - e^{i\delta_8}}{3\sqrt{2}}P^{\text{eff}}_{t-c}.$$

The amplitudes for the charge-conjugate modes are identical, except for the understood CKM coefficients. Decay amplitudes for B_S mode are

$$\mathcal{A}\left(B_S \to K^-\pi^+\right)$$

$$= \frac{3e^{i\delta_8} + 2e^{i\delta_{27}}}{5}T - \frac{2\left(e^{i\delta_8} - e^{i\delta_{27}}\right)}{5}C + e^{i\delta_8}P^{\text{eff}}_{t-c},$$

$$\mathcal{A}\left(B_S \to \bar{K}^0\pi^0\right)$$

$$= -\frac{3\left(e^{i\delta_8} - e^{i\delta_{27}}\right)}{5\sqrt{2}}T + \frac{2e^{i\delta_8} + 3e^{i\delta_{27}}}{5\sqrt{2}}C - \frac{e^{i\delta_8}}{\sqrt{2}}P^{\text{eff}}_{t-c},$$

$$\mathcal{A}\left(B_S \to \bar{K}^0\eta_8\right)$$

$$= -\frac{3\left(e^{i\delta_8} - e^{i\delta_{27}}\right)}{5\sqrt{6}}T + \frac{2e^{i\delta_8} + 3e^{i\delta_{27}}}{5\sqrt{6}}C - \frac{e^{i\delta_8}}{\sqrt{6}}P^{\text{eff}}_{t-c},$$

$$\mathcal{A}(B_S \to K^+K^-)$$

$$= \frac{5 + 8e^{i\delta_8} + 7e^{i\delta_{27}}}{20}T - \frac{5\left(1 - e^{i\delta_8}\right) + 21\left(e^{i\delta_8} - e^{i\delta_{27}}\right)}{60}C$$

$$+ \frac{2 + e^{i\delta_8}}{3}P^{\text{eff}}_{t-c},$$

$$\mathcal{A}(B_S \to K^0\bar{K}^0)$$

$$= \frac{5\left(1 - e^{i\delta_8}\right) + \left(e^{i\delta_8} - e^{i\delta_{27}}\right)}{20}T$$

$$- \frac{5\left(1 - e^{i\delta_8}\right) - 3\left(e^{i\delta_8} - e^{i\delta_{27}}\right)}{60}C + \frac{2 + e^{i\delta_8}}{3}P^{\text{eff}}_{t-c},$$

$$\mathcal{A}(B_S \to \pi^+\pi^-)$$

Table 7. Fit results for direct CP-asymmetries (A_{CP})

Direct CP-asymmetry A_{CP} (%)			$SU(3)$-elastic				On-shell $c\bar{c}$			
			Table 1		Table 2		Table 3		Table 4	
$\Delta S = 0$		Exp.	60°	90°	60°	90°	60°	90°	60°	90°
B_S	$\overline{K^0}\eta_8$	–	−78	−99	−88	−70	−32	−19	−72	−36
	$\overline{K^0}\pi^0$	–	−78	−99	−88	−70	−32	−19	−72	−36
	$K^-\pi^+$	–	23	25	19	26	23	22	26	31
B^+	$\pi^+\eta_8$	–	49	60	28	41	23	27	27	35
	$\overline{K^0}K^+$	–	−71	−64	−67	−56	−32	−19	−33	−24
	$\pi^+\pi^0$	-7 ± 15	0	0	0	0	0	0	0	0
B^0	K^+K^-	–	14	16	11	18	–	–	–	–
	$K^0\overline{K^0}$	–	−88	−95	−87	−58	−32	−19	−33	−24
	$\eta_8\eta_8$	–	−96	−98	−16	39	−32	−19	22	33
	$\pi^0\eta_8$	–	0	0	0	0	−32	−19	−33	−24
	$\pi^+\pi^-$	38 ± 27	42	54	43	42	23	22	26	31
	$\pi^0\pi^0$	–	−49	−70	−69	−85	−32	−19	−72	−36
$\Delta S = 1$		Exp.	60°	90°	60°	90°	60°	90°	60°	90°
B^0	$K^0\eta_8$	–	10	12	9.5	11	1.2	1.1	5.5	5.9
	$K^0\pi^0$	3 ± 37	10	12	9.5	11	1.2	1.1	5.5	5.9
	$K^+\pi^-$	-9.3 ± 2.9	−7.5	−7.7	−6.1	−6.4	−6.1	−5.5	−6.7	−7.0
B^+	$K^+\eta_8$	–	19	23	18	22	7.4	7.6	13	15
	$K^+\pi^0$	1 ± 12	−15	−15	−11	−12	−6.1	−5.5	−9.1	−9.8
	$K^0\pi^+$	1 ± 6	3.4	3.9	2.9	3.4	1.2	1.1	1.3	1.3
B_S	K^+K^-	–	−12	−16	−13	−11	−6.1	−5.5	−6.7	−7.0
	$K^0\overline{K^0}$	–	5.0	7.9	4.7	3.6	1.2	1.1	1.3	1.3
	$\eta_8\eta_8$	–	8.1	11	9.5	8.7	1.2	1.1	3.3	3.5
	$\pi^0\eta_8$	–	0	0	−80	−71	–	–	0	0
	$\pi^+\pi^-$	–	−1.4	−1.3	−0.9	−1.3	–	–	–	–
	$\pi^0\pi^0$	–	−1.4	−1.3	−0.9	−1.3	–	–	–	–

Table 8. Fit results for the time-dependent CP-asymmetry parameter $S_{f\bar{f}}$

$S_{f\bar{f}}$ (%)			$SU(3)$-elastic				On-shell $c\bar{c}$			
			Table 1		Table 2		Table 3		Table 4	
$\Delta S = 0$		Exp.	60°	90°	60°	90°	60°	90°	60°	90°
B^0	K^+K^-	–	−99	−83	−99	−90	–	–	–	–
	$K^0\overline{K^0}$	–	−30	2.3	−27	−5.2	−19	−10	−24	−16
	$\eta_8\eta_8$	–	−23	−18	−49	−36	−19	−10	−97	−86
	$\pi^0\eta_8$	–	6.2	−1.2	6.2	−1.2	−19	−10	−24	−16
	$\pi^+\pi^-$	-58 ± 34	−69	16	−67	−1.3	−81	−6.5	−81	−9.7
	$\pi^0\pi^0$	–	−67	8.4	−39	51	−19	−10	65	86

$$= \frac{5\left(1-e^{i\delta_8}\right)+\left(e^{i\delta_8}-e^{i\delta_{27}}\right)}{20}T$$
$$- \frac{5\left(1-e^{i\delta_8}\right)-3\left(e^{i\delta_8}-e^{i\delta_{27}}\right)}{60}C + \frac{2\left(1-e^{i\delta_8}\right)}{3}P^{\text{eff}}_{t-c},$$

$$\mathcal{A}(B_S \to \pi^0\pi^0)$$
$$= \frac{5\left(1-e^{i\delta_8}\right)+\left(e^{i\delta_8}-e^{i\delta_{27}}\right)}{20\sqrt{2}}T$$
$$- \frac{5\left(1-e^{i\delta_8}\right)-3\left(e^{i\delta_8}-e^{i\delta_{27}}\right)}{60\sqrt{2}}C + \frac{2\left(1-e^{i\delta_8}\right)}{3\sqrt{2}}P^{\text{eff}}_{t-c},$$

$$\mathcal{A}\left(B_S \to \pi^0\eta_8\right)$$
$$= \frac{3\left(e^{i\delta_8}-e^{i\delta_{27}}\right)}{5\sqrt{3}}T - \frac{2e^{i\delta_8}+3e^{i\delta_{27}}}{5\sqrt{3}}C,$$

$$\mathcal{A}\left(B_S \to \eta_8\eta_8\right)$$
$$= \frac{5\left(1-e^{i\delta_8}\right)+9\left(e^{i\delta_8}-e^{i\delta_{27}}\right)}{20\sqrt{2}}T$$
$$- \frac{5+8e^{i\delta_8}+27e^{i\delta_{27}}}{60\sqrt{2}}C + \frac{2\left(1+e^{i\delta_8}\right)}{3\sqrt{2}}P^{\text{eff}}_{t-c}.$$

Table 9. Experimental situation and averages as mentioned in the text

	Belle [5]	BaBar [6]	Average
$A_{\pi^+\pi^-}$	$0.77 \pm 0.27 \pm 0.08$	$0.19 \pm 0.19 \pm 0.05$	0.38 ± 0.27
$S_{\pi^+\pi^-}$	$-1.23 \pm 0.41 \pm 0.08$	$-0.40 \pm 0.22 \pm 0.03$	-0.58 ± 0.34

Finally, assuming negligible $PP, D\bar{D} \rightleftharpoons D^*\bar{D}^*, D^{**}\bar{D}^{**}, ...$, the $B \to D\bar{D}$ decay amplitudes are

$$\begin{aligned}
\mathcal{A}\left(B^+ \to D_s^+ \bar{D}^0\right) &= \mathcal{A}\left(B^0 \to D_s^+ D^-\right) \\
&= \mathrm{e}^{\mathrm{i}\delta_8^D} T_D, \\
\mathcal{A}\left(B^+ \to D^+ \bar{D}^0\right) &= \mathcal{A}\left(B_S \to D^+ D_s^-\right) = \mathrm{e}^{\mathrm{i}\delta_8^D} T_D, \\
\mathcal{A}\left(B^0 \to D^+ D^-\right) &= \frac{1}{3}\mathrm{e}^{\mathrm{i}\delta_8^D}\left(2 + \mathrm{e}^{-\mathrm{i}\delta_8}\right) T_D, \\
\mathcal{A}\left(B^0 \to D^0 \bar{D}^0\right) &= -\mathcal{A}\left(B^0 \to D_s^+ D_s^-\right) \\
&= \frac{1}{3}\mathrm{e}^{\mathrm{i}\delta_8^D}\left(1 - \mathrm{e}^{-\mathrm{i}\delta_8}\right) T_D, \\
\mathcal{A}\left(B_S^0 \to D_s^+ D_s^-\right) &= \frac{1}{3}\mathrm{e}^{\mathrm{i}\delta_8^D}\left(2 + \mathrm{e}^{-\mathrm{i}\delta_8}\right) T_D, \\
\mathcal{A}\left(B_S \to D^0 \bar{D}^0\right) &= -\mathcal{A}\left(B_S \to D^+ D^-\right) \\
&= \frac{1}{3}\mathrm{e}^{\mathrm{i}\delta_8^D}\left(1 - \mathrm{e}^{-\mathrm{i}\delta_8}\right) T_D.
\end{aligned}$$

C Fit results for branchings and asymmetries

The experimental data on B to two pseudoscalar decays we shall use are summarized in Tables 5 and 6, where direct CP-asymmetries are defined according to the sign convention:

$$A_{CP} = \frac{\Gamma\left(\bar{B} \to \bar{f}\right) - \Gamma\left(B \to f\right)}{\Gamma\left(\bar{B} \to \bar{f}\right) + \Gamma\left(B \to f\right)}. \tag{46}$$

An average is made over CLEO [1], Belle [2] and BaBar [3] measurements (see also [4]), assuming no correlation. The implications of $SU(3)$ symmetry bear on the decay amplitudes, so predictions for branchings must be corrected for to account for lifetime differences and available phase-space. From [22], the lifetime correction factor is $\Gamma_{\mathrm{tot}}\left(B^+\right)/\Gamma_{\mathrm{tot}}\left(B^0\right) = 0.92$, while that of phase space is of at most a few percents and can be neglected. The branchings under brackets in Table 6 are branching fractions for the physical η state and not for η_8, so that they are only indicative. Indeed, the small admixture of singlet η_0 into the physical η state could lead to large effects. The last observables of interest to us are the time-dependent asymmetry parameters

$$\begin{aligned}
A_{f\bar{f}} &= \frac{\left|\lambda_{f\bar{f}}\right|^2 - 1}{\left|\lambda_{f\bar{f}}\right|^2 + 1} = A_{CP}, \\
S_{f\bar{f}} &= \frac{2\mathrm{Im}\lambda_{f\bar{f}}}{\left|\lambda_{f\bar{f}}\right|^2 + 1},
\end{aligned}$$

with

$$\lambda_{f\bar{f}} = \mathrm{e}^{-2\mathrm{i}\beta}\frac{A\left(\bar{B} \to f\bar{f}\right)}{A\left(B \to f\bar{f}\right)}. \tag{47}$$

The experimental situation and averages are (with inflated errors; see [22]) as in Table 9.

We have used only $A_{\pi^+\pi^-} = -C_{\pi^+\pi^-}$ as input.

The function we minimize to find the best-fit values is as usual

$$\chi^2 = \sum_f \left(\frac{\mathrm{Br}^{\mathrm{th}} - \mathrm{Br}^{\mathrm{exp}}}{\sigma_{\mathrm{Br}}^{\mathrm{exp}}}\right)^2 + \sum_f \left(\frac{A_{CP}^{\mathrm{th}} - A_{CP}^{\mathrm{exp}}}{\sigma_{A_{CP}}^{\mathrm{exp}}}\right)^2, \tag{48}$$

where the sum runs over measured decay branchings and asymmetries (twelve inputs). Upper bounds are implemented using the arc-tangent representation of the step function (three inputs).

Finally, the Wolfenstein parameterization [24] of the CKM matrix elements is used:

$$V_{\mathrm{CKM}} = \tag{49}$$
$$\begin{pmatrix}
1 - \frac{\lambda^2}{2} - \frac{\lambda^4}{8} & \lambda & A\lambda^3\left(\rho - \mathrm{i}\eta\right) \\
-\lambda & 1 - \frac{\lambda^2}{2} - \left(\frac{A^2}{2} + \frac{1}{8}\right)\lambda^4 & A\lambda^2 \\
A\lambda^3\left(1 - \rho - \mathrm{i}\eta\right) & -A\lambda^2 + A\lambda^4\left(\frac{1}{2} - \rho - \mathrm{i}\eta\right) & 1 - \frac{A^2\lambda^4}{2}
\end{pmatrix},$$

and we take the central values of [22]:

$$\begin{aligned}
\lambda = 0.2196 \pm 0.0023, \quad A = 0.854 \pm 0.045, \\
\sqrt{\rho^2 + \eta^2} = 0.43 \pm 0.07,
\end{aligned} \tag{50}$$

and we keep only the weak angle $\gamma = \arctan \eta/\rho$ as a free parameter (so unitarity of V_{CKM} is implied). For the parameter $S_{f\bar{f}}$, we use the average $\sin 2\beta = 0.736 \pm 0.049$ extracted from charmonium modes [25].

The results of the fits for branchings and asymmetries are collected in Tables 6 to 8. Column labels refer to the best-fit parameter tables given in the text.

References

1. CLEO Collaboration (S. Chen et al.), Phys. Rev. Lett. **85**, 525 (2000); D.M. Asner et al., Phys. Rev. D **65**, 031103 (2002); A. Bornheim et al., hep-ex/0302026
2. BELLE Collaboration (K. Abe et al.): T. Tomura, presented at the 38th Rencontres de Moriond, March 22–29, 2003, Les Arcs, France, hep-ex/0305036; contributed paper to the XXI International Symposium on Lepton and Photon Interactions at High Energies, Fermilab, August, 11–16, 2003, hep-ex/0308040

3. BABAR Collaboration (B. Aubert et al.), Phys. Rev. Lett. **89**, 281802 (2002); contributed to Flavor Physics and CP Violation (FPCP), Philadelphia, Pennsylvania, 16–18 May 2002, hep-ex/0206053; contributed to 31st International Conference on High Energy Physics, Amsterdam, The Netherlands, July 24–31, 2002, hep-ex/0207065; Phys. Rev. Lett. **91**, 021801 (2003); M. Bona, talk given at the 2003 Flavor Physics and CP Violation, Paris, June 3–6, 2003, BABAR-TALK-03065; J. Ocariz, presented at the International Europhysics Conference on HEP (EPS2003), Aachen, July 17–23, 2003, BABAR-TALK-03083; hep-ex/0308012
4. John Fry, talk at the XXI International Symposium on Lepton and Photon Interactions at High Energies, Fermilab, August 11–16, 2003
5. BELLE Collaboration (K. Abe et al.), Phys. Rev. D **68**, 012001 (2003)
6. BABAR Collaboration (B. Aubert et al.), preliminary result presented at the XXI International Symposium on Lepton and Photon Interactions at High Energies, Fermilab, August 11–16, 2003, BABAR-PLOT- 0054
7. R. Fleischer, T. Mannel, Phys. Rev. D **57**, 2752 (1998); M. Gronau, J.L. Rosner, Phys. Rev. D **57**, 6843 (1998); R. Fleischer, Eur. Phys. J. C **6**, 451 (1999); Phys. Lett. B **435**, 221 (1998); M. Neubert, J.L. Rosner, Phys. Lett. B **441**, 403 (1998); Phys. Rev. Lett. **81**, 5076 (1998); M. Neubert, JHEP **9902**, 014 (1999); A.J. Buras, R. Fleischer, Eur. Phys. J. C **11**, 93 (1999); C **16**, 97 (2000); R. Fleischer, J. Matias, Phys. Rev. D **61**, 074004 (2000); J. Matias, Phys. Lett. B **520**, 131 (2001); M. Bargiotti et al., Eur. Phys. J. C **24**, 361 (2002); M. Gronau, J.L. Rosner, Phys. Rev. D **65**, 013004 (2002); R. Fleischer, J. Matias, Phys. Rev. D **66**, 054009 (2002); A.I. Sanda, K. Ukai, Prog. Theor. Phys. **107**, 421 (2002); M. Neubert, talk given at International Workshop on Heavy Quarks, Leptons, Salerno, Italy, 27 May–1 June 2002, hep-ph/0207327; Y.-Y. Keum, hep-ph/0209208; R. Fleischer, Proceedings of International School on Heavy Quark Physics, Dubna, Russia, 27 May–5 June 2002, hep-ph/0210323; Z.-J. Xiao, C.-D. Lu, L. Guo, hep-ph/0303070; M. Gronau, J.L. Rosner, hep-ph/0307095; M. Beneke, M. Neubert, hep-ph/0308039; Z.-Z. Xing, hep-ph/0308225; A. Buras, R. Fleischer, S. Recksiegel, F. Schwab, hep-ph/0309012
8. J. de Swart, Rev. Mod. Phys. **35**, 916 (1963); D. Zeppenfeld, Z. Phys. C **8**, 77 (1981); M. Savage, M. Wise, Phys. Rev. D **39**, 3346 (1989); L.-L. Chau, H.-Y. Cheng, W.K. Sze, H. Yao, B. Tseng, Phys. Rev. D **43**, 2176 (1991)
9. M. Gronau, O. Hernandez, D. London, J. Rosner, Phys. Rev. D **50**, 4529 (1994); D **52**, 6356 (1995); D **52**, 6374 (1995)
10. C. Smith, Eur. Phys. J. C **10**, 639 (1999)
11. K.M. Watson, Phys. Rev. **88**, 1163 (1952)
12. J.-M. Gérard, C. Smith, Eur. Phys. J. C **30**, 69 (2003)
13. J.-M. Gérard, W.-S. Hou, Phys. Rev. Lett. **62**, 855 (1989); Phys. Rev. D **43**, 2909 (1991)
14. W.-S. Hou, K.-C. Yang, Phys. Rev. Lett. **84**, 4806 (2000); C.-K. Chua, W.-S. Hou, K.-C. Yang, Mod. Phys. Lett. A **18**, 1763 (2003)
15. D. Delepine, J.-M. Gérard, J. Pestieau, J. Weyers, Phys. Lett. B **429**, 106 (1998); J.-M. Gérard, J. Pestieau, J. Weyers, Phys. Lett. B **436**, 363 (1998)
16. J.D. Bjorken, Nucl. Phys. Proc. Suppl. **11**, 325 (1989); M.J. Duncan, B. Grinstein, Phys. Lett. B **255**, 583 (1991); H.D. Politzer, M.B. Wise, Phys. Lett. B **257**, 399 (1991)
17. M. Beneke, G. Buchalla, M. Neubert, C.T. Sachrajda, Nucl. Phys. B **606**, 245 (2001)
18. G. 't Hooft, Nucl. Phys. B **72**, 461 (1974); A.J. Buras, J.-M. Gérard, R. Ruckl, Nucl. Phys. B **268**, 16 (1986)
19. J.-M. Gérard, J. Weyers, Eur. Phys. J. C **7**, 1 (1999); M. Neubert, Phys. Lett. B **424**, 152 (1998)
20. L.M. Sehgal, M. Wanninger, Z. Phys. C **50**, 47 (1991); A.N. Kamal, Phys. Rev. D **60**, 094018 (1999); Z. Xing, Phys. Lett. B **493**, 301 (2000)
21. S. Barshay, G. Kreyerhoff, JHEP **0309**, 004 (2003)
22. Particle Data Group Collaboration (K. Hagiwara et al.), Phys. Rev. D **66**, 010001 (2002)
23. CLEO Collaboration (S. Ahmed et al.), Phys. Rev. D **66**, 031101 (2002)
24. L. Wolfenstein, Phys. Rev. Lett. **51**, 1945 (1983)
25. BABAR Collaboration (B. Aubert et al.), Phys. Rev. Lett. **89**, 201802 (2002); BELLE Collaboration (K. Abe et al.), contributed to the XXI International Symposium on Lepton and Photon Interactions at High Energies, Fermilab, August 11–16, 2003, hep-ex/0308036